

A modified Pile Load Test Based on Numerical and Experimental Evaluation of Bored Pile in Clayey Soil

طريقة معدلة لاختبار التحميل الاستاتيكي على خوازيق الحفر بناء على تقييم سلوك الخازوق في التربة الطينية بالطرق العددية والمعملية

Bakr R., Ibrahim A., and Elmeligy M.

Faculty of Engineering, Mansura University, Mansoura, Dakahleya, Egypt

ملخص:

هذه الورقة تلخص دراسة عن تقييم اختبار التحميل الاستاتيكي كاداة للتنبؤ بسلوك الخازوق في التربة الطينية. تم عمل محاكاة للحالات المختلفة للتربة والخازوق باستخدام ثلاثة نماذج تأسيسية مختلفة هي: نموذج موهر كولمب ونموذج تصلب التربة ونموذج زحف التربة اللينة. كما تم محاكاة سيناريوهات اختبار التحميل الاستاتيكي ايضا لدراسة سلوك الخازوق. تم تحليل هذه النماذج بواسطة الطرق العددية لحل العناصر المحددة باستخدام برنامج بلاكسيس ثلاثي الابعاد للاساسات. تم اختيار موقع بمدينة المنصورة بمحافظة الدقهلية بجمهورية مصر العربية لاجراء الاختبارات الحقلية. لعمل محاكاة للتربة بالنماذج المذكورة تم تنفيذ جستن بعقم 25 متر لدراسة خصائص التربة في الموقع المذكور حيث تم اجراء اختبارات التحميل به لاحقا. تم حساب قدرة الخازوق والهبوط المتوقع لكل حالة نظريا باستخدام معادلات الكود المصري والنماذج التأسيسية. تم عمل محاكاة لاختبار التحميل مرتين لكل حالة. الاولى تحاكي طريقة الاختبار القياسية والثانية تحاكي طريقة التحميل الحقيقي. نتائج الدراسة توضح ان سلوك الخازوق اثناء اختبار التحميل الاستاتيكي القياسي مبالغ فيه للغاية. تم اقتراح طريقة معدلة لاختبار التحميل وتحقيقتها. واثبتت الدراسة ان الطريقة المعدلة المقترحة يمكن استخدامها كبديل افضل من الطريقة الحالية.

ABSTRACT:

This study summarizes the evaluation of the pile static load test as a tool for the prediction of pile behavior in clayey soils. The pile and soil cases were modeled by three different constitutive models; Mohr-Columb (M-C), Hardening Soil (HS), and Soft Soil Creep (SSC). The static loading test scenarios were also numerically modeled to study the pile behavior. The models were analyzed by using numerical finite elements software (PLAXIS 3D Foundation). A construction site located in Mansoura, Dakahleya Governorate, EGYPT, was selected to perform the field tests. In order to simulate the soil in the numerical models, two borings with depth of 25 m were carried out to investigate the soil properties in the same site where field static pile load tests are performed later. The pile capacity and settlement were calculated theoretically for each case by using both Egyptian Code formula and numerical constitutive models. The load test was simulated twice for each pile. The first simulates the standard static load test while the second simulates the real-life loading. The results showed that the pile behavior obtained by standard static load test was extremely exaggerated. A modified quick static load test method was proposed and verified. Also it has been proved that, the Modified Quick Load Test (MQLT) method can be used as an alternative method to the classical static load test method.

1 INTRODUCTION:

The current pile design practice is still mainly based on empirical approximate methods whose design parameters are often obtained from field and laboratory tests. The pile loading capacity is generally defined as the load for which rapid and substantial movement occurs under slight increase of the applied load, Bengt H. Fellenius (2001). For pile

foundation projects, it is usually required to confirm the pile capacity and to verify that the pile behavior agrees with the design assumptions. The most acceptable method to verify that is the static loading test. On most occasions, a distinct ultimate load is not achieved in the test therefore the pile capacity can be predicted by some methods based on the load-movement data recorded during the

test. In clayey soils, it is noted that, the pile capacity determined from the theoretical formulas differs greatly from that determined from the static loading test since the time-dependent pile behavior cannot be accurately predicted from the current static load test procedure. It is widely accepted that a pile transfers its load into the surrounding soil through two mechanisms; friction and adhesion along the pile shaft-soil interface as well as end-bearing through the pile base, Meyerhof (1976), Briaud (1985), Aoki and De'Alencar (1975), Shioi and Fukui (1982), Bazaraa and Kurkur (1986). Many attempts have been made to reliably predict the pile capacity contributions but unfortunately, owing to the complicated mechanism of pile-soil interaction, none of these methods can accurately predict the pile behavior. In Egypt, Delta region has emerged as one of heavily populated urban cities in the world. Due to the rapid economic growth, multi storied buildings have been constructed. Construction industry is further challenged in many cases by the sub-soil conditions due to the presence of thick stiff to very stiff clay as top strata. In many cases, sand layers of 4 to 6 meter exist at depth from 10 to 20 meter confined between the clay layers. Due to these constraints, design of pile foundation becomes infeasible if the upper layers are neglected and piles are extended into the deeper sand layers which are often found at depths of 20 to 40 meters. The current static load test method in most building codes does not differentiate between clay and granular soil despite the apparent disparity in their mechanical properties as well as the pile behavior in clay is different from that in sand. Therefore, the main objective of this study is the evaluation of the current static load method as a tool for the prediction of pile behavior and the development of a new method accurately reflecting the pile behavior in clayey soil in a more accurate way.

2 MODELING THEORIES:

Predicting the response of piles to axial loads in a finite element analysis requires a soil constitutive model that accurately captures pile-soil interaction. Several soil constitutive numerical models have been developed to date and most of them are available for finite element analysis. Lade (2005) prepared a summary of widely available soil constitutive models. Moore and Brachman (1994) conducted linear-elastic soil models while Fernando and Carter (1998) conducted nonlinear models including nonlinear elastic models, perfectly plastic models, and plastic models with hardening. Modeling Soil behavior during failure in three-dimensional state of stress is extremely complicated. The basic components for material models are simply represented by few basic types of soil constitutive models. The elastic-plastic Mohr-Coulomb model (M-C) involved five input parameters, i.e. modulus of elasticity (E) and Poisson's ratio (ν) for soil elasticity; angle of internal friction (ϕ) and cohesion (c) for soil plasticity and angle of dilatancy (ψ). Although the increase of stiffness with depth can be taken into account, the Mohr-Coulomb model does neither include stress dependency nor stress-path dependency of stiffness or anisotropic stiffness. In contrast to the Mohr-Coulomb model, the Hardening Soil (HS) model has been presented as a hyperbolic model with non-linear stress-strain relationship and stress-dependency of stiffness moduli (Lee and Salgado, 1999). The limiting states of stress are described in HS by means of ϕ , c , and ψ . However, soil stiffness is described much more accurately by using three different input stiffness: the triaxial loading stiffness, E_{50} , the triaxial unloading stiffness, E_{ur} , and the odometer loading stiffness, E_{oed} . Time-dependent behavior of clayey soil can be attributed to two reasons; the consolidation and the inherent viscous characteristics of the soil skeleton which can be considered as strain rate time-dependent. Creep, relaxation, rate

sensitivity and secondary compression and also common approaches in Viscoplasticity theory are discussed by Oka (1999). Unlike elastic materials, soft soil loses energy if a load is applied and then removed. Time-dependent behavior is first modeled by an empirical relation based on experimental results observed in a creep test and a relaxation test. Garlanger (1972) proposed a compression model by including the secondary compression term. The explicit introduction of time violates the principle of objectivity in continuum mechanics, (Eringen 1962). Consequently, this type of empirical relation is one-dimensional strictly limited to the specific boundary and loading conditions (Singh & Mitchell, 1968). Murayama & Shibata (1964) proposed a rheology model based on the rate process theory. Adachi and Okano (1974) proposed an elasto-viscoplastic constitutive model that extends the critical state energy, (Roscoe et al 1963). Viscoplasticity theory is relatively simple extension of viscoelastic model where permanent strain is observed. Oka (1999) and Adachi & Oka (1982) assumed that normally consolidated clay never reaches the static equilibrium state even at the end of primary consolidation, and viscoplastic strain is taken as a hardening parameter. The secondary compression is most dominant in soft soils, i.e. normally consolidated clays, silts and peat which can be well described by the Soft Soil Creep model (SSC), (Brinkgreve, 1994).

3 SOIL PROFILE:

A construction site located in Mansoura, Dakahleya Governorate, Egypt is selected to perform the field tests. In order to investigate the soil properties in the same site where field static pile load tests are carried out later two boreholes with depth 25 m are carried out. Representative soil samples are taken from each borehole and laboratory tests are performed to determine the soil properties for each layer. The water table is encountered at depth 2.00 meter from the existing ground

level. Description of soil layers and their properties are shown in Fig. (1).

4 CASES OF STUDY:

In order to study the factors affecting the pile behavior in clay soil, two models were numerically created. The first model-pile is relatively short with $l/d = 10$ where it is extended in the upper clay layer to depth 6.50 meter. The other model-pile is relatively long with $l/d = 41$ where it is penetrating multi-layered soil and extended in the lower clay layer to depth 22.00 meter. Where l and d are pile length and diameter respectively. Accordingly, the pile lengths for both the first and the second cases are 5.00 and 20.50 meter respectively. Diameter of all piles used in the simulation is 50 cm.

5 ESTIMATION OF PILE STATIC CAPACITY AND TEST LOADS:

The Formulas of the Egyptian Code of Practice for deep foundation (ECP-202/2001) were used to estimate the pile capacity and the corresponding settlement for both cases. The pile capacity obtained from ECP-202/2001 was verified by using the numerical analysis software (Plaxis -3D Foundation). Table (1) presents the values of the estimated pile capacity and the settlement for both cases.

Table 1 Pile Static Capacity and Settlement by ECP-202/2001

Case	Pile Length m	Q_s kN	Q_b kN	Q_u kN	S_s mm	S_{pp} mm	S_{ps} mm	S_t mm
1	5	223	67	290	0.2	19.6	10.2	30.1
2	20.5	1250	54.8	1305	4.7	19.6	21.8	46.0

Where; Q_s , Q_b , Q_u , S_s , S_{pp} , S_{ps} , and S_t are shaft resistance, toe resistance, pile ultimate capacity, elastic compression, settlement due to end-bearing, settlement due to shaft resistance, and total settlement.

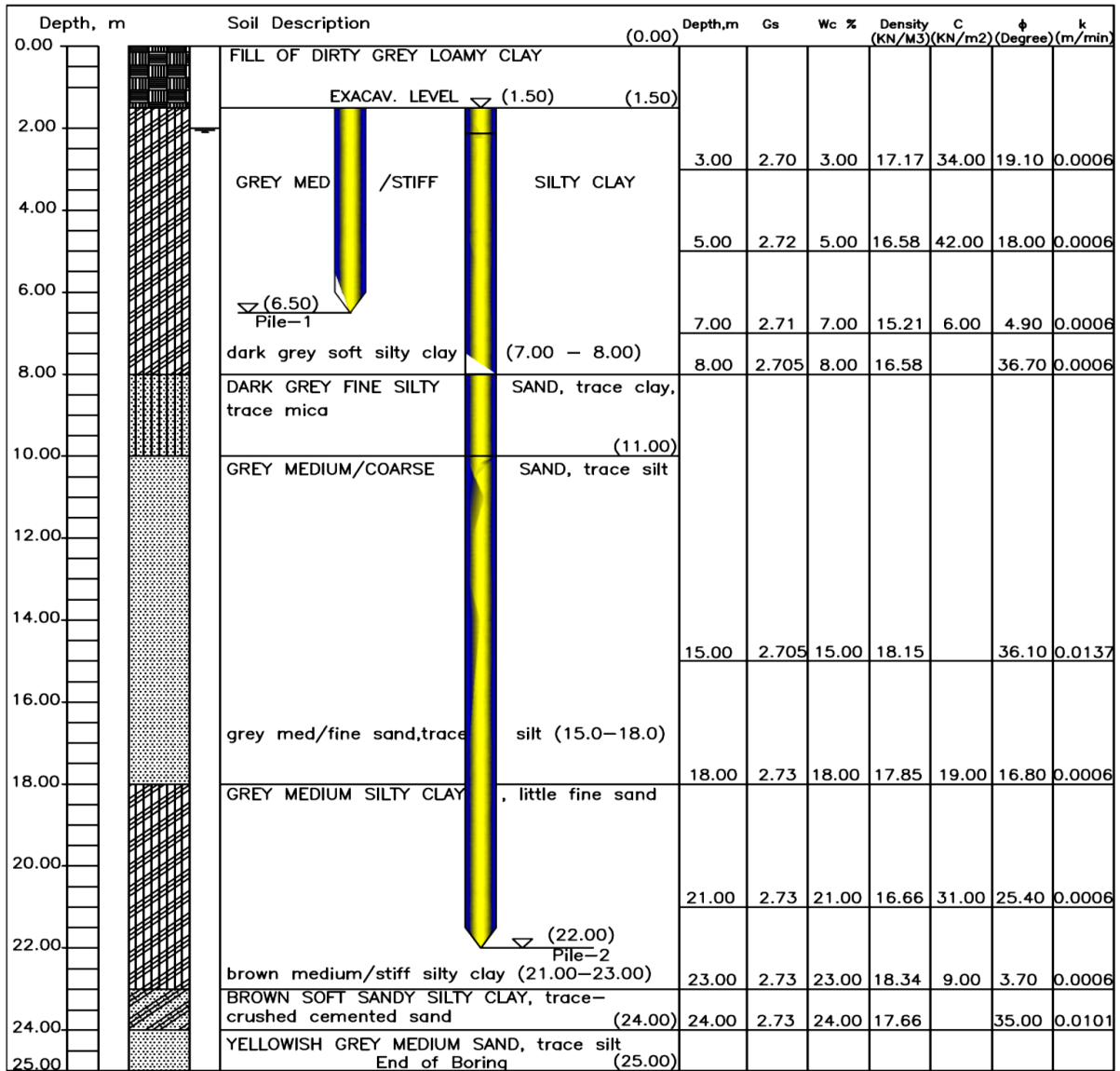


Fig. (1) Borehole Log

According to ECP-202/2001:

- The design loads can be obtained by dividing the ultimate pile capacity calculated from the theoretical static formula including the earthquake loads by factor of safety (2.0).
- The test load is calculated by multiplying the design load by factor 1.5.

Table (2) presents the magnitude of ultimate and test loads.

Table 2 Pile Capacity and Test Loads

Case	l/d	Q _u kN	Q _d kN	Q _{t1} kN	Q _{t2} kN
1	10	290	145	218	145
2	41	1305	653	979	653

Where, Q_d, Q_{t1}, and Q_{t2} are ultimate pile capacity, design load, test load for SSLT, and test load for RLL.

6 MODEL SIMULATION:

The numerical simulation for field static load tests was carried out on the assigned test piles twice. The first test represents the standard

static load test (SSLT) while the other test represents the real-life loading (RLL) which is defined by the author as the actual permanent loading procedure during the building life period. The pile behavior obtained from both simulations is compared to find out whether the current SSLT realistically represent the actual pile behavior or not. The simulation was performed by using three constitutive models M-C, HS, and SSC models with drained condition to predict the final settlement and undrained to predict the static load test settlement. The models analysis is carried out by the finite element code (Plaxis 3D Foundation manual Version 2). The undrained soil condition option is selected in order to represent the case of saturated clayey soil subjected to a quick loading. To study the pile time dependent behavior, a consolidation calculation step is performed following each plastic loading step for a consolidation time equal to the corresponding time in the real load test for both M-C and HS models while SSC model is self-time-dependent.

6.1 Simulation of case-1

6.1.1 Simulation of SSLT

This model is analyzed by each of M-C, HS, and SSC models. For the static test load simulation, the soil is assumed undrained and a consolidation step is assigned following to the plastic calculation step. The test load (218 kN) is divided into 6 equal increments/decrements and maintained for the specified periods. Fig. (2) portrays a comparison for the pile behavior represented by the pile total resistance versus total settlement predicted by the three models. Fig. (3) and Fig. (4) portrays the shaft and toe resistances for the same simulation case while respectively.

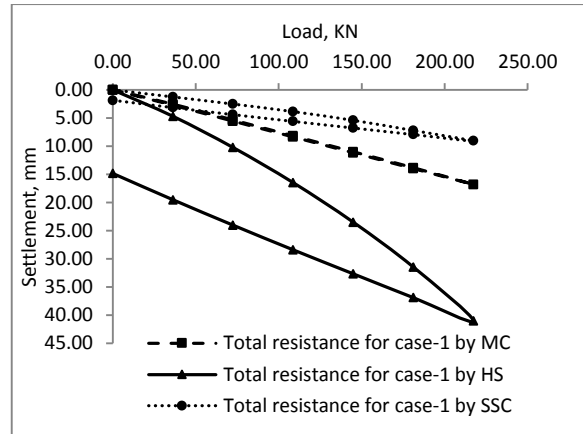


Fig. (2) Pile total resistance Vs. total settlement by SSLT for case-1.

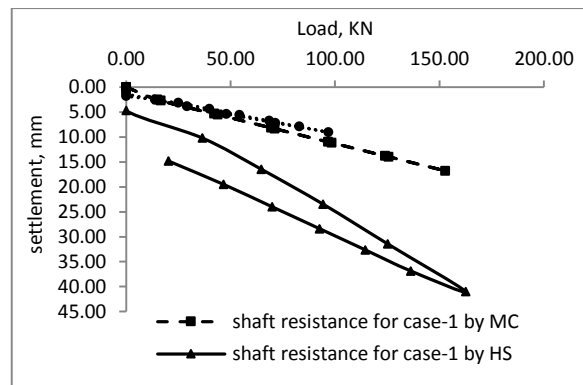


Fig. (3) Shaft resistance Vs. settlement by SSLT for case-1.

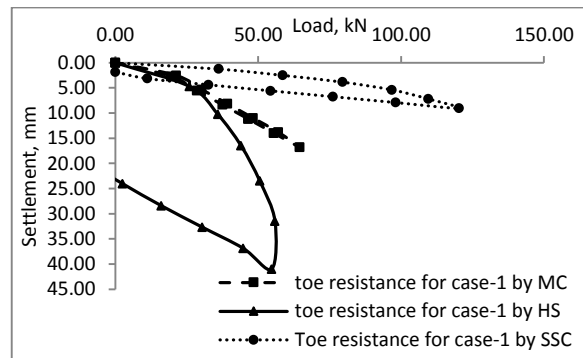


Fig. (4) Toe resistance Vs. settlement by SSLT for case-1.

Table (3) presents the analysis results obtained from M-C, HS, and SSC models including total settlement, shaft, toe, and total pile resistance.

Table 3 Analysis results for case-1 by SSLT

Model	Q_u kN	Q_s kN	Q_b kN	S_t mm
M-C	218	153	65	16.80
HS	218	163	55	41.00
SSC	218	97	121	9.05

From the analysis by M-C we get; approximately linear relationship follows almost the same path in both loading and unloading. Moreover, upon the completion of the unloading procedure, no permanent deformation remained therefore the pile behavior can be considered almost linear elastic. The toe resistance represents 29.67% of the total pile capacity while shaft resistance represents 70.33%. Since the pile is too short, so the elastic compression of the pile represents negligible percentage and most of the head displacement occurs due to the settlement in the soil. The toe resistance which mobilizes first, increases quickly at the beginning of loading and continues to increase, but at a lower rate until the end of the loading. On the contrary, the shaft resistance starts later and then increases at a higher rate until the end of the loading. From the literature, the undrained behavior of clay soil causes the applied load is carried first by pore water then transferred gradually to the soil. The consolidation process during which the load is transferred to the soil needs a more time depending on the soil permeability.

From the analysis by HS we get; the permanent deformation is 14.84 mm. The pile behavior can be considered nonlinear elastic-plastic with hardening. The toe resistance represents 25.17% of the total pile capacity while shaft resistance represents 74.83%. As mentioned for the M-C analysis, the elastic compression of the pile represents negligible percentage and most of the head displacement occurs due to the settlement in the soil. The toe resistance which mobilizes first, increases quickly at the beginning of loading and continues to increase, but at a lower rate until the end of the loading. On the contrary, the shaft resistance mobilizes later than the toe resistance but it rapidly increases and continues increasing until the end of the loading. The consolidation settlement continued increasing at the end of the loading period, i.e., the maintaining period for the full

factored load is not sufficient to cover the full consolidation.

From the analysis by SSC model The toe and shaft resistances represent 55.38% and 44.62% of the total load respectively. The pile behavior can be described as non-linear plastic. The permanent deformation is 1.84mm representing 20% of the total settlement. The toe resistance which mobilizes first, increases quickly at the beginning of loading and continues to increase, but at a lower rate until the end of the loading. On the contrary, the shaft resistance mobilizes at settlement 1.25mm then increases linearly with approximately constant rate to the end of the loading. The consolidation settlement continue increasing to the end of the loading period, i.e., the maintaining period for the full factored load is not sufficient to cover the full consolidation. Comparing the results obtained from HS and M-C with that obtained from SSC analysis it can be concluded that, the settlement obtained by SSC is significantly lower than that obtained by M-C (53.87%) and extremely lower than that obtained by HS analysis (22.06%). Pile behavior by M-C is linear elastic while it is nonlinear plastic by both HS and SSC models.

6.1.2 *Simulation of RLL for case-1*

The test load (145 kN) is divided into 7 increments, six of them represent the dead load (80% of the working load) and the seventh increment (20% of the working load) represents the live load to simulate the real-life loading procedure. The construction period for each loading increment is assumed 60 days while it is assumed 7 days for each demolishing decrement. The building design life time is assumed to be 50 years. The soil boundary condition is assumed drained. Fig. (5) portrays a comparison for the pile behavior represented by the pile total resistance versus total settlement predicted by the three models. Fig. (6) and Fig. (7) portrays the shaft and toe resistances for the same simulation case while respectively.

Table 4 presents the analysis results for RLL by using all simulation models including total pile capacity, shaft resistance, toe resistance, and total settlement occurred.

Table 4 Analysis results for case-1 by RLL

Model	Q_u kN	Q_s kN	Q_b kN	S_t mm
M-C	145	43	102	12.61
HS	145	48	97	25.50
SSC	145	89	56	6.38

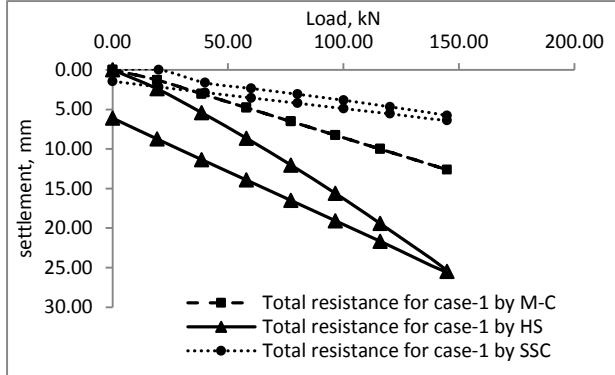


Fig. (5) Pile total resistance Vs. total settlement by RLL for case-1.

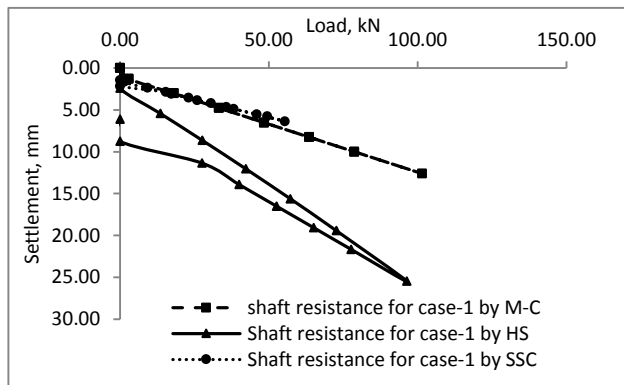


Fig. (6) Shaft resistance Vs. settlement by RLL for case-1.

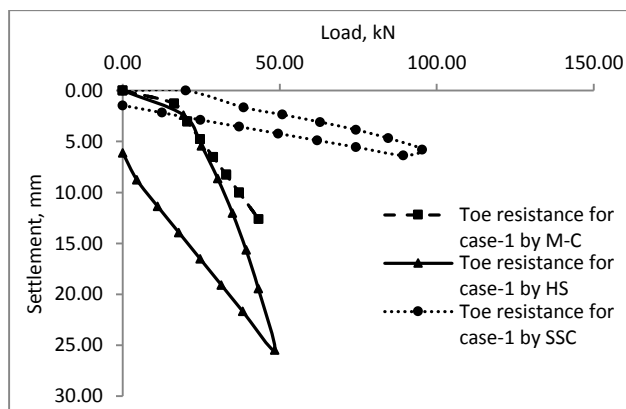


Fig. (7) Toe resistance Vs. settlement by RLL for case-1.

From the analysis by M-C model the toe and the shaft resistances represent 29.9% and 70.1% of the total applied load respectively. The toe resistance which mobilizes first representing most of the pile resistance, increased constantly to the end of loading. The shaft resistance which mobilizes later than the toe resistance continues increasing to the end of loading.

From the analysis by HS model; the permanent deformation is 6.13 mm. The toe resistance is 48.38 kN representing 33.4% of the total resistance. Shaft resistance is 96.45 kN representing 66.6% of the total pile load. The pile behavior is slightly nonlinear elastic-plastic. The toe resistance mobilizes first representing most of the pile resistance up to settlement of 2.50 mm then shaft resistance mobilizes and continued increasing to the end of loading. The consolidation occurring after the loading completion over the building life period is 1.25 mm.

From the analysis by SSC model, the toe and shear resistances represent 61.71% and 38.29% of the total test load respectively. The permanent deformation is 1.45 mm representing 22.73% of the total settlement. The pile behavior may be divided into two phases. In both phases, the pile behavior is linear but with higher deformation rate in the first phase. The second phase started approximately at load 40 kN. The pile resistance increases linearly but with higher rate in the second phase due to the soil hardening. The pile length is relatively short therefore the toe resistance contribution represents most of the pile resistance. The toe resistance also mobilizes faster than the shaft resistance. The pile behavior may be described as two-phase linear plastic.

6.1.3 Comparing Pile Behavior in Case-1 by SSLT and Real-Life

A comparison between the results obtained from the analysis of the numerical models which simulate pile loading by both standard static load test and real-life are shown in Fig. (8).

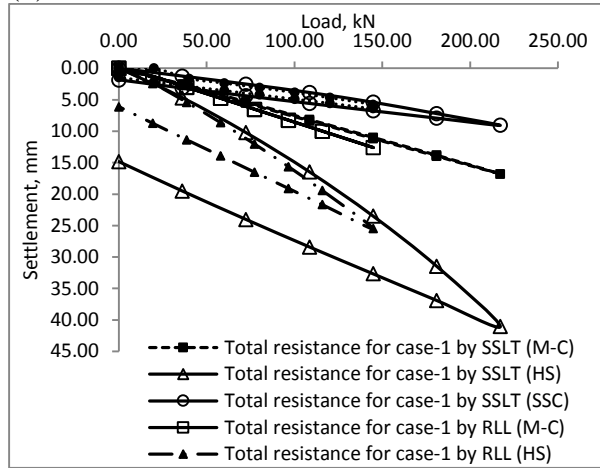


Fig. (8) Comparison between SSLT and RLL for case-1

The SSC model produced the lowest settlement over all the models (5.58 mm and 9.23 mm) followed by M-C model (12.41 mm and 16.80 mm) in both cases of loading SSLT and real-life respectively. HS produced the highest settlement (24.94 mm and 41.02 mm) by SSLT and real-life loading respectively. The highest shaft resistance (124.06 kN) in real-life loading is produced by M-C while it is (162.57 kN) by HS in SSLT. The highest toe resistances (95.35 kN and 120.33 kN) are obtained by SSC in real-life and SSLT respectively.

6.2 Simulation of case-2

Pile-soil model for case-2 is also numerically simulated once according to standard static load test and again simulated according to real-life loading procedure. The models are analyzed by the same way as for case-1 under the same conditions. The pile capacity and the working loads are 1304.89 kN and 652.44 kN respectively.

6.2.1 Simulation of SSLT

The test load, (979 kN), is divided into 6 equal increments/decrements and maintained for the specified periods. A comparison portrays the pile behavior predicted by the three models is shown in Fig. (9). Figs. (10) and (11) show the relationship between shaft and toe resistance with the total settlement respectively.

Table (5) presents the analysis results for all simulation models including; ultimate pile capacity, shaft resistance, toe resistance, and total settlement for case-2.

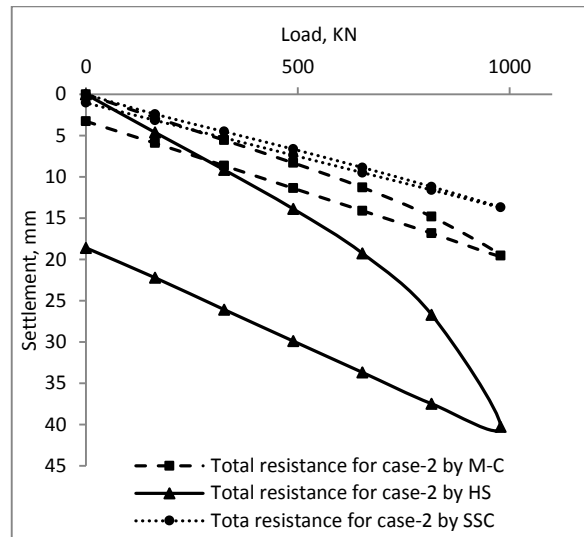


Fig. (9) Pile resistance Vs. settlement by SSLT for case-2

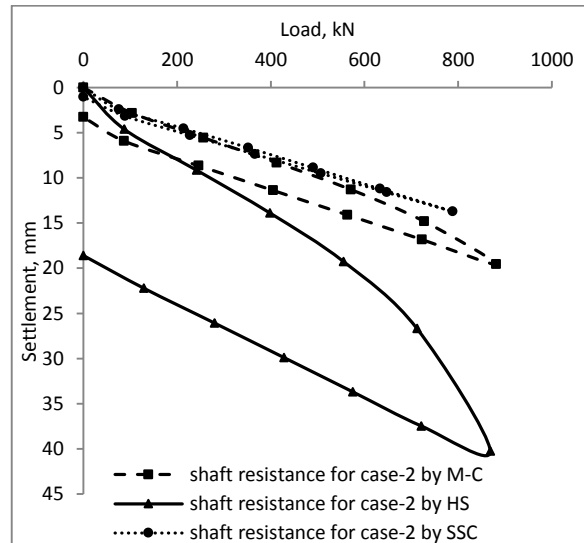


Fig. (10) Shaft resistance Vs. Settlement by SSLT for case-2

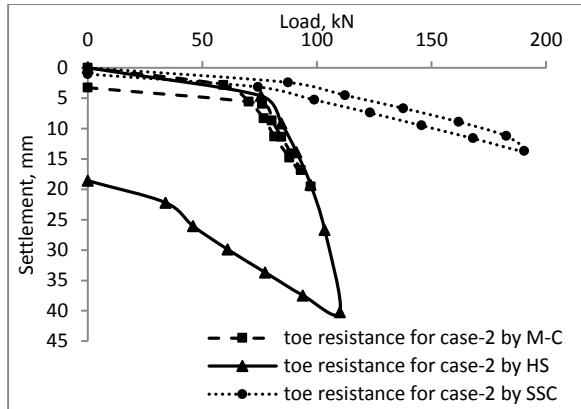


Fig. (11) Toe resistance Vs. Settlement by SSLT for case-2

Table 5 Analysis results for case-2 by SSLT

Model	Q_u kN	Q_s kN	Q_b kN	S_t mm
M-C	979	881	98	19.54
HS	979	868	111	41.32
SSC	979	788	191	13.7

From the analysis by M-C model; the shaft and the toe resistances represent 90% and 10% of the total test load respectively. The permanent settlement after removal of the full load is 3.27 mm. The pile behavior can be described as linear up to 100% design load then becomes non-linear plastic. There is a consolidation settlement 1.53 mm occurring during the last load maintaining period (12 hrs.) but it remains constant during the last 5 hours.

From the analysis by HS model; the toe resistance represent 11.30 % while shaft resistance represent 88.7% of the total factored load. The permanent deformation is 18.60 mm. The consolidation settlement during maintaining period of the total factored load is 4.46 mm. At the end of loading period, the settlement continue increasing, therefore more settlement would be expected. The pile behavior can be described nonlinear elastic-plastic with hardening.

From the analysis by SSC model; The shaft and the toe resistances represent 80.5% and 19.5% of the total pile resistance respectively. The permanent deformation remained after removal of the full applied load is 1.04 mm. The pile behavior is slightly non-linear plastic.

6.2.2 Simulation of RLL

Figs. (12) to (14) show the relationship between the total pile capacity, the shaft resistance, and the toe resistance with the total settlement for case-2 when simulated according to RLL scenario. The working load (653 kN) is applied in 7 increments. Six equal increments. Table (6) presents the analysis results for case-2 according to RLL.

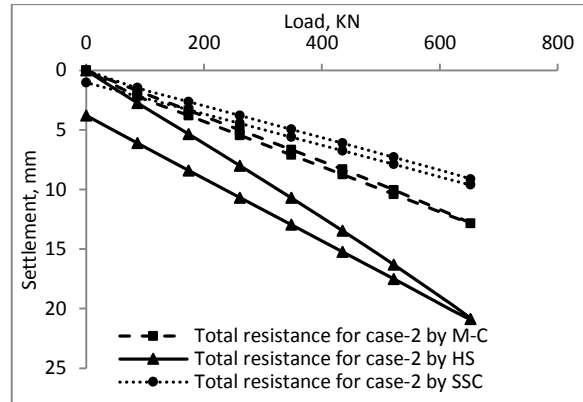


Fig. (12) Pile resistance Vs. Settlement by RLL for case-2

From the analysis by M-C model; The toe resistance represents 12.2% while shaft resistance represents 87.8% of the design load. No permanent deformation is remained upon removal of the applied load. The pile behavior can be divided into two stages the first is linear and the second stage which starts at 435 kN is non-linear.

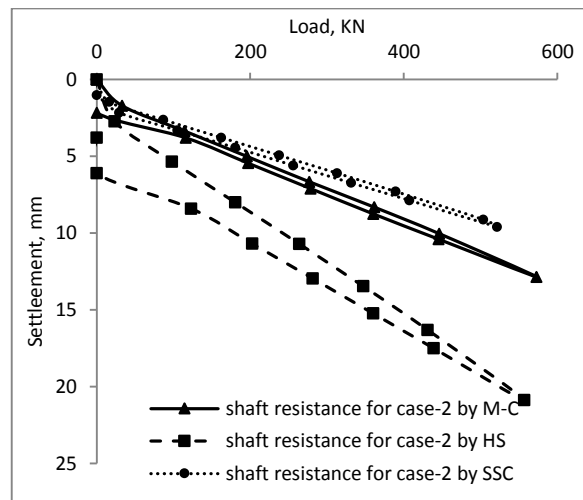


Fig. (14) Shaft resistance Vs. Settlement by RLL for case-2

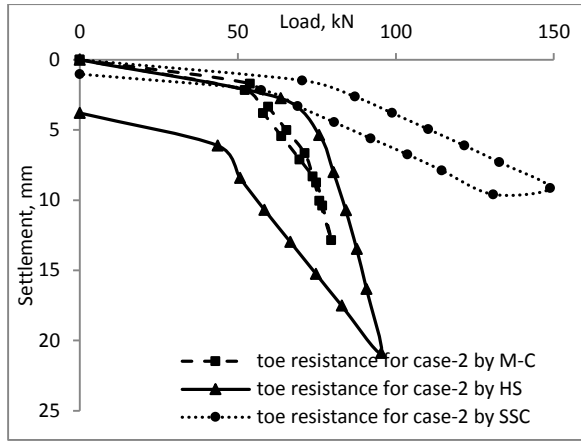


Fig. (14) Toe resistance Vs. Settlement by RLL for case-2

Table 6 Analysis results for case-2 by RLL

Model	Q_u kN	Q_s kN	Q_b kN	S_t mm
M-C	653	573	80	12.85
HS	653	653	95	20.88
SSC	653	522	131	9.60

Therefore pile behavior can be considered linear-non-linear elastic. The toe resistance mobilizes first with slightly higher resistance than the shaft resistance but it quickly changes to be almost constant whereas the shaft resistance continues increasing to the end of loading. The consolidation settlement occurs during the design life time after the completion of loading is 2.81 mm.

From the analysis by HS model; The toe resistance represents 14.61% while shaft represents 85.39%. The permanent deformation is 3.79 mm. The consolidation during the period of full load application is 5 mm approximately. The toe resistance which mobilizes first increases faster than the shaft resistance but it decays quickly while shaft resistance continue increasing up to the end of loading. The pile behavior can be described as linear elastic-plastic.

From the analysis by SSC model; the permanent settlement after removal of the test load is 1.02 mm. The shaft resistance contribution represents 80% while the toe resistance represent 20% of the total test load. The consolidation settlement during the building life period is 0.5 mm. The pile

behavior is almost linear slightly plastic except during the last load increment. It can be noted that upon the completion of pile loading and during the remaining design life time, the shaft resistance is increased from 503.62 kN to 521.62 kN. On the contrary, the toe resistance is decreased from 148.83 kN to 130.83 kN although the total applied load is constant during this period.

6.2.3 Comparing Pile Behavior in Case-2 by SSLT and Real-Life

The pile behavior relationships as obtained by M-C, HS, and SSC models according to SSLT and RLL are shown in Fig. (15).

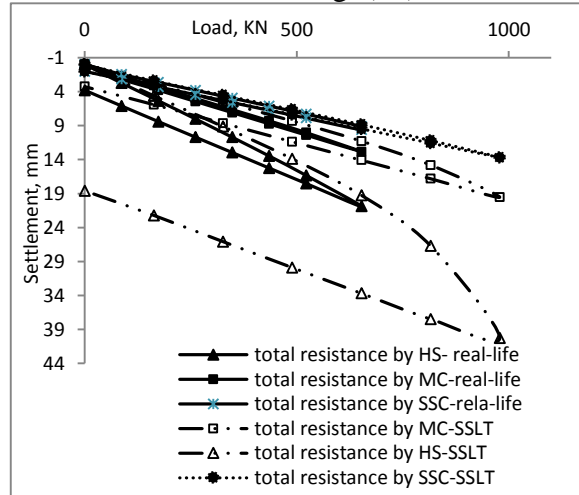


Fig. (15) Comparison of Pile Behavior for case-2 by SSLT and RLL

The SSC model produces the lowest settlement over all the models (13.7 mm and 9.13 mm) followed by M-C model (19.54 mm and 12.85 mm) in both cases of loading SSLT and real-life respectively. HS produces the highest settlement in both cases (40.26 mm and 20.88 mm) respectively. From Fig. (11), the highest shaft resistance is produced by M-C analysis (881.37 kN and 572.85 kN) followed by HS (868.66 kN and 557.11 kN) in both cases SSLT and real-life respectively. The lowest shaft resistance (788.12 kN and 521.62 kN) in both cases is obtained by the SSC model. Unlike the shaft resistance, the toe resistance produced by SSC analysis is the highest (190.54 kN and 9.13 kN) followed by HS model (110 kN and 95.34 kN) in both

cases of loading; ECP and real-life respectively. The lowest toe resistance (97.29 kN and 79.6 kN) in both cases are obtained by M-C analysis. The total settlements obtained by real life loading represents 65.76%, 51.86%, and 66.64%, of those obtained by SSLT when analyzed by M-C, HS, and SSC respectively.

7 MODIFICATIONS TO SSLT

From the previous analysis, it can be noted that, performing static loading tests by applying factored loads with factor of 1.5 or higher according to the current method of static load test caused an unrealistic exaggerated image about the time-dependent pile behavior. Therefore, the current static load test method should be modified or replaced by another more realistic. The Authors suggest some modifications to the standard static loading test to be more reliable, less expensive, and requiring shorter time. To achieve the proper modifications to the current static load test method, numerical analysis is again performed but with different scenarios of loading unloading, and maintaining time periods. The analysis is also performed by M-C, HS and SSC models to capture the proper simulation of the real-life pile behavior. The results show that the following modifications may be implemented to the current test method (SSLT):

1. The design load is calculated by dividing the reliable pile ultimate capacity by 2 in case of taking the earthquake loads into consideration.
2. Utilizing a load factor of 1.1 instead of 1.5 or higher to be multiplied by the design load to calculate the test load.
3. The number of load increments is changed to be 5 instead of 6.
4. The load increments represent; 0.25, 0.25, 0.25, 0.25, 0.1 of the design load respectively.
5. The time periods of load increments are also changed to be 0.5, 0.5, 1.0,

1.0, 2.0 hours for loading and 0.15, 0.15, 0.15, 0.15, and 2.0 hours for unloading consuming a total test period of 8 hours compared with 26.25 hours in the standard static load test method.

7.1 Simulation of Case-1

The ultimate pile capacity, working load, and test load are 289.67, 144.83, and 159.32 kN respectively. The same pile-soil model for the previous upper clay case is used in this analysis.

Figs. (16) to (18) show comparison between the pile behavior obtained from the simulation according to both RLL and MQLT methods by using the three constitutive models; M-C, HS, and SSC respectively. Tables (7) to (9) presents the load components and the corresponding settlements obtained by simulating both RLL and MQLT by M-C, HS, SSC for case-1 respectively.

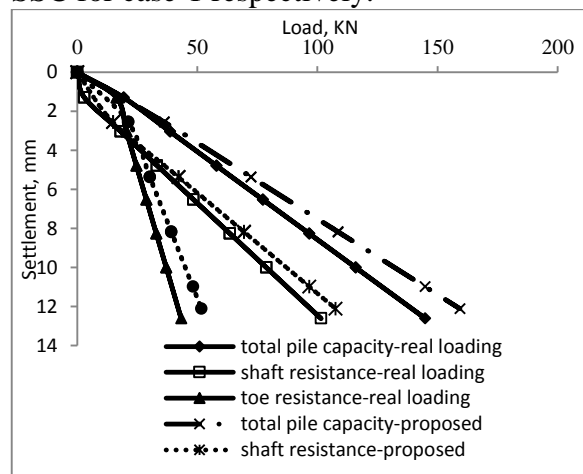


Fig. (16) MQLT & real-Life by M-C for case-1.

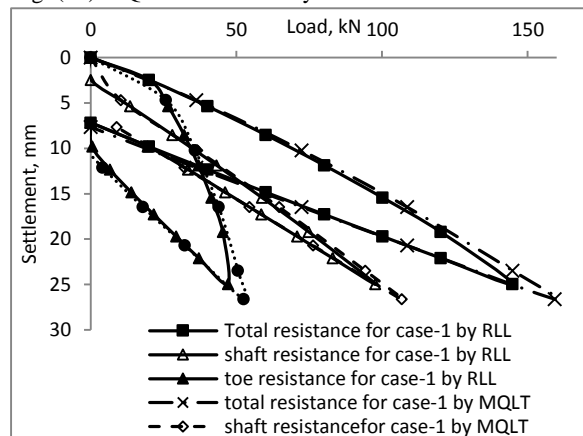


Fig. (17) MQLT & Real-Life by HS for case-1.

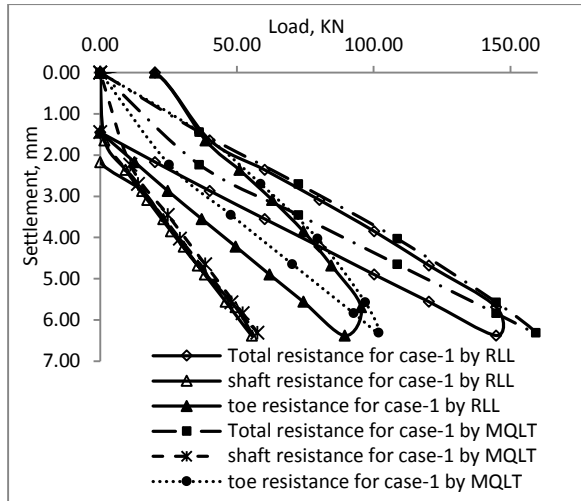


Fig. (18) MQLT & real-Life by SSC for case-1.

Table 7 Results of RLL & MQLT for case-1 by M-C

Method	Q_t kN	Q_s kN	Q_b kN	S_t mm
RLL	145	102	43	12.61
MQLT	160	108	52	12.12

Table 8 Results of RLL & MQLT for case-1 by HS

Method	Q_t kN	Q_s kN	Q_b kN	S_t mm
RLL	145	97	48	25.48
MQLT	160	107	53	26.60

Table 9 Results of RLL & MQLT for case-1 by SSC

Method	Q_t kN	Q_s kN	Q_b kN	S_t mm
RLL	145	56	89	6.38
MQLT	160	58	102	6.31

From the analysis by M-C model; the test load is 10% higher than the real life load therefore the shaft and toe resistances calculated by modified load test model are also consequently higher. The increase in toe resistance (19.5%) is higher than that occurred in shaft resistance (6.2%). No permanent deformation remained upon completion of unloading process. The pile behavior predicted by both real-life and modified loading is linear elastic.

From the analysis by HS model; the permanent deformation is 7.66 mm which represent about 28.8% of the total settlement. The pile behavior predicted by both real-life and modified loading is elastic-plastic slightly

nonlinear. From the analysis by SSC model; the shaft and toe resistances represent 36.06% and 63.95% in MQLT compared with 38.29% and 61.71% in RLL. The permanent deformation obtained by MQLT is negligible compared with that obtained by real-life loading (1.44 mm).

7.2 Simulation of Case-2

The ultimate pile capacity, design load, and test load are 1305, 653, and 718 kN respectively. The same pile-soil model for case-1 is used in this analysis. Figs. (19) to (21) show the relationships between pile resistance contributions and the total settlement from both test methods RLL and MQLT by M-C, HS, and SSC respectively.

Tables (10) to (12) presents the load components and the corresponding settlements obtained by simulating both RLL and MQLT by M-C, HS, SSC for case-2 respectively.

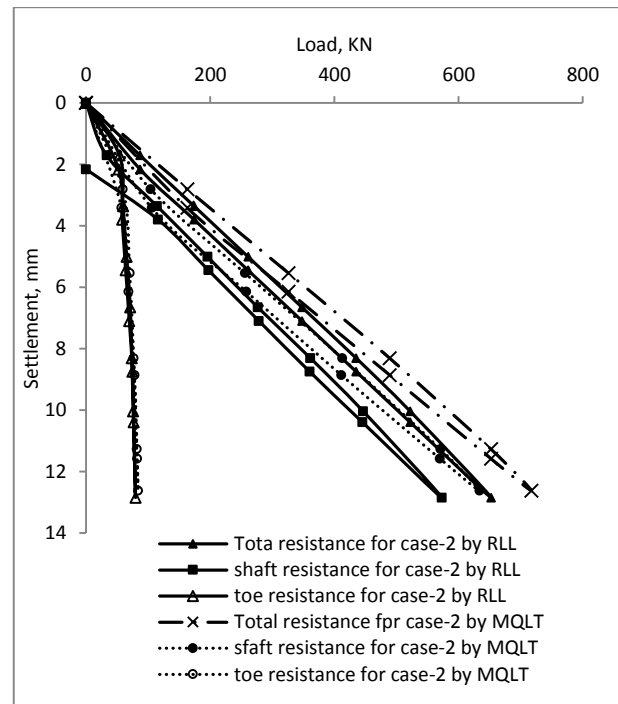


Fig. (19) MQLT & Real-Life by M-C for case-2.

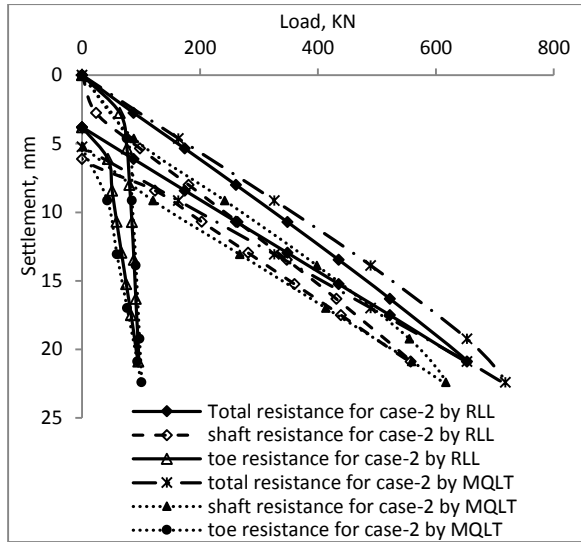


Fig. (20) MQLT & Real-Life by HS for case-2.

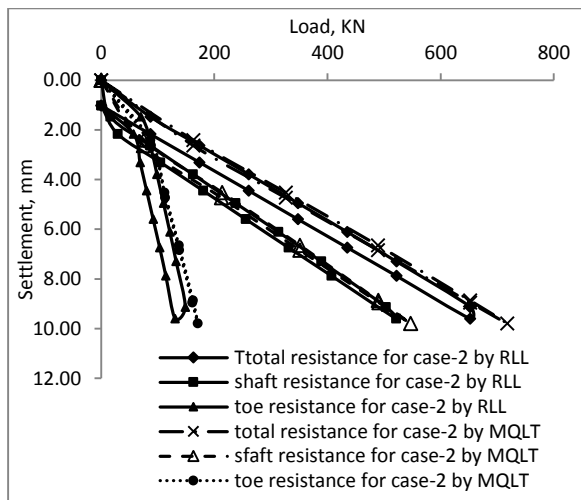


Fig. (21) MQLT & real-Life by SSC for case-2.

Table 10 Results of RLL & MQLT for case-2 by M-C

Method	Q_t kN	Q_s kN	Q_b kN	S_t mm
RLL	653	573	80	12.85
MQLT	718	634	84	12.62

Table 11 Results of RLL & MQLT for case-2 by HS

Method	Q_t kN	Q_s kN	Q_b kN	S_t mm
RLL	653	558	95	20.88
MQLT	718	617	101	22.41

Table 12 Results of RLL & MQLT for case-2 by SSC

Method	Q_t kN	Q_s kN	Q_b kN	S_t mm
RLL	653	522	131	9.60
MQLT	718	547	171	9.79

From the analysis by M-C model; the toe and shaft resistances obtained from MQLT represent 23.80% and 76.20 % from the test load corresponding to 20.10% and 79.90% by RLL. The MQLT test load is 10% higher than the RLL therefore the shaft and toe resistances calculated by modified load test model are also consequently higher. No permanent deformation remained upon completion of unloading process. The pile behavior predicted by both real-life and modified loading is slightly nonlinear elastic.

From the analysis by HS model; the shaft and the toe resistances obtained by MQLT represent 85.9% and 14.1% of the test load corresponding to 85.5% and 14.5% by MQLT. The permanent deformation is 5.22 mm which represent about 23.3% of the total settlement. The pile behaviors predicted by both RLL and MQLT are elastic-plastic slightly nonlinear.

From the analysis by SSC model; The shaft and toe resistances represent 76.19% and 23.81% by MQLT corresponding to 79.95% and 20.05% by RLL. The permanent deformation after removal of the full load is negligible by MQLT compared with 1.02 mm by real-life.

8 CONCLUSIONS:

From the numerical simulation by MC, HS, and SSC for both cases; upper and lower clay, it can be concluded that:

- It has been proved that, the real pile behavior can not be represented by the standard static load test method because of the exaggerated load factor.
- The pile behavior can be more accurately represented by MQLT method in both cases of upper and lower clay whether analysis is performed by M-C, or HS, or SSC.
- It can be concluded that the SSC model is better than both M-C and HS models in the prediction of pile behavior in clayey soils.

REFERENCES:

- Adachi, T., Oka, F., 1982. Constitutive equation for normally consolidated clays based on elasto-Viscoplasticity, *Soils and Foundations* 22: Pp. 57-70.
- Aoki, N. and De'Alencar, D. 1975. An approximate method to estimate the bearing capacity of Piles, *Proceeding of the Fifth Pan-American Conference on Soil Mechanics and Foundation Engineering*, Buenos Aires, Argentina, pp. 367-376.
- Bazaraa, A. R. & Kurkur, M. M. 1986. N-values used to predict settlements of piles in Egypt, *Proceedings of in Situ '86*, New York, pp. 462-474.
- Briaud, J. L. and Tucker, L. M. 1988 Measured and predicted axial capacity of 98 piles, *Journal of Geotechnical Engineering*, ASCE, Vol. 114, No. 9, pp. 984-1001.
- Bengt H. Fellenius 2001. Determining the true distribution of load in piles, International Deep Foundation Congress, Geotechnical Special Publication No. 116.
- Brinkgreve, R.B.J., 1994. Geometrical Models and Numerical Analysis of Softening, *Dissertation*. Delft University of Technology.
- Fernando, N. S. M. and Carter, J. P. 1998. Elastic Analysis of Buried Pipes under Surface patch Loadings, *Journal of Geotechnical and Geoenvironmental Engineering*, Vol. 124, No. 8, pp. 720-728.
- Egyptian Code of Practice for Deep Foundations (ECP-202-2001), Vol.4, Ver. 2011.
- Eringen, C. 1962. Non-linear theory of continuous media, McGraw Hill.
- Garlanger, J.E. (1972) "*The consolidation of soils exhibiting creep under constant Effective stress*", *Geotechnique*, Vol. 22, No.1, pp 71-78.
- Lade, P. V. (2005), "*Overview of Constitutive Models for Soils*," *Soil Constitutive Models—Evaluation, Selection, and Calibration*, J. A. Yamamuro and V. N. Kaliakin, Eds., ASCE, Reston, VA, pp. 1-34.
- Lee, Salgado, 1999.
- Meyerhof, G. G. (1976) "*Bearing capacity and settlement of pile foundations*" The Eleventh Terzaghi Lecture, ASCE Journal of Geotechnical Engineering, Vol. 102, Iss. GT3, pp. 195-228.
- Moore, I. D. and Brachman, R. W. (1994), "*Three-Dimensional Analyses of Flexible Circular Culverts*." *Journal of Geotechnical Engineering*, Vol. 120, No. 10, pp. 1829-1844.
- Murayama, S and Shibata, T. (1964) "*Flow and stress relaxation of clays*." IUTAM symp On Rheology and Soil Mechanics, Grenoble, pp 99-129.
- Oka, F. (1999) "*Continuum theory of granular materials*." An Introduction Mechanics of Granular Materials. Oda, M & Iwashita, K, editors. Balkema, Netherlands, pp 107-113.
- Plaxis 3D Foundation Manual, Version 2.
- Roscoe, KH, Schofield, AN and Thrairajah, A. (1963) "*Yielding of clays in states wetter than critical*." *Geotechnique*, Vol.13, No.3, pp 211-240.17.
- Singh & Mitchell, (1968).Bolton, M.D. 1986. The strength and dilatancy of sands. *Geotechnique*, 36(1): 65 - 78.